INVESTIGATING THE ABILITY TO PREHEAT AND IGNITE ENERGETIC MATERIALS USING ELECTRICALLY CONDUCTIVE MATERIALS

A Thesis

Submitted to the Faculty

of

Purdue University

by

Marlon D. Walls, Jr.

In Partial Fulfillment of the

Requirements for the Degree

of

Master of Science in Mechanical Engineering

August 2020

Purdue University

West Lafayette, Indiana

THE PURDUE UNIVERSITY GRADUATE SCHOOL
STATEMENT OF THESIS APPROVAL

Dr. Jeffrey F. Rhoads, Chair

School of Mechanical Engineering

Dr. Steven F. Son

School of Mechanical Engineering

Dr. George T.-C. Chiu

School of Mechanical Engineering

Approved by:

Dr. Nicole Key

Head of the School of Mechanical Engineering Graduate Program

ACKNOWLEDGMENTS

First and foremost, I would like to thank God for giving me the mental strength to persevere and mature during my time at Purdue. I'd like to thank my advisor, Dr. Jeffrey Rhoads, for his guidance in learning to think independently as a researcher. I also would like to thank my research group for their continuous support despite my initial ignorance in various areas, and especially Dr. Trevor Fleck for his various contributions to my research from before I arrived in Indiana until the day I finished.

I would not have made it this far without my supporting cast. Special thanks to my parents and sisters who have supported me in every decision I've made for myself. Thanks to my extended family: Granny, Aunte, Uncle Dixson, Uncle Phil, Uncle Jones, and other family members who have supported me from afar during my journey. Much appreciation goes out to the communities of supporters I've built all across the country along my journey, including those in Michigan, Texas, Maryland, Indiana and California; it truly does take a village. Lastly, I would like to thank my *fiancée* for sticking with me despite my physical absence over the past 2.5 years. Thankfully FaceTime was there to help mitigate the effects of enduring the long distance relationship.

This research was supported in part by Purdue University, as well as by the U.S. Department of Defense, Defense Threat Reduction Agency through grant No. HDTRA1-15-1-0010, which is managed by Dr. Jeffrey Davis. The content of the information does not necessarily reflect the position or the policy of the U.S. federal government, and no official endorsement should be inferred.

TABLE OF CONTENTS

Page

LIST OF TABLES

LIST OF FIGURES

Figure Page

ABSTRACT

Walls, Jr., Marlon D. M.S.M.E., Purdue University, August 2020. Investigating the Ability to Preheat and Ignite Energetic Materials Using Electrically Conductive Materials. Major Professor: Jeffrey F. Rhoads, School of Mechanical Engineering.

The work discussed in this document seeks to integrate conductive additives with energetic material systems to offer an alternative source of ignition for the energetic material. By utilizing the conductive properties of the additives, ohmic heating may serve as a method for preheating and igniting an energetic material. This would allow for controlled ignition of the energetic material without the use of a traditional ignition source, and could also result in easier system fabrication.

For ohmic heating to be a viable method of preheating or igniting these conductive energetic materials, there cannot be significant impact on the energetic properties of the energetic materials. Various mass solids loadings of graphene nanoplatelets (GNPs) were mixed with a reactive mixture of aluminum (Al)/polyvinylidene fluoride (PVDF) to test if ohmic heating ignition was feasible and to inspect the impact that these loadings had on the energetic properties of the Al/PVDF. Results showed that while ohmic heating was a plausible method for igniting the conductive energetic samples, the addition of GNPs degraded the energetic properties of the Al/PVDF. The severity of this degradation was minimized at lower solids loadings of GNPs, but this consequently resulted in larger voltage input requirements to ignite the conductive energetic material. This was attributable to the decreased conductivities of the samples at lower solids loading of GNPs.

In hopes of conserving the energetic properties of the Al/PVDF while integrating the conductive additives, additive manufacturing techniques, more specifically fused filament fabrication, was used to print two distinct materials, Al/PVDF and a conductive composite, into singular parts. A CraftBot 3 was used to selectively deposit

Conductive Graphene PLA (Black Magic) filament with a reactive filament comprised of a PVDF binder with 20% mass solids loadings of aluminum. Various amounts of voltage were applied to these conductive energetic samples to quantify the time to ignition of the Al/PVDF as the applied voltage increased. A negative correlation was discovered between the applied voltage and time to ignition. This result was imperative for demonstrating that the reaction rate could be influenced with the application of higher applied voltages.

Fused filament fabrication was also used to demonstrate the scalability of the dual printed conductive energetic materials. A flexural test specimen made of the Al/PVDF was printed with an embedded strain gauge made of the Black Magic filament. This printed strain gauge was tested for dual purposes: as an igniter and as a strain sensor, demonstrating the multi-functional use of integrating conductive additives with energetic materials.

In all, the experiments in this document lay a foundation for utilizing conductive additives with energetic materials to offer an alternative form of ignition. Going forward, ohmic heating ignition may serve as a replacement to current, outdated methods of ignition for heat sensitive energetic materials.

1. INTRODUCTION

1.1 Background

As the evolution of energetic material technology has progressed, a need for an innovative design to reliably initiate, ignite, and preheat the energetic materials has developed. Energetic materials (EMs) typically fall into one of three categories: propellants, explosives, or pyrotechnics [1]. These EMs have a wide range of applications ranging from military utilization in large caliber ammunition systems, to civil applications, including airbags in motor vehicles [2].

The term 'igniter' generally refers to a device that prompts the deflagration, or burning, of an EM through a heat stimulus, such as a flame, or electrical induction through a hot wire. However, if this deflagration results in a shockwave formation, the reaction is then termed as a detonation and the process is instead referred to as an initiation [3]. Initiators, or detonators, are devices that enable the detonation of EM. These initiators are commonly used with primary explosives that are sensitive to stimuli such as impact, friction, heat or spark. Oftentimes, triggering sequences, or explosive trains, are necessary to initiate secondary high explosives and propellants [1]. In these applications, primers, which typically contain small amounts of primary explosives, are often used as the first component of the explosive train. The detonation of the primary explosive produces a high energy shockwave which results in the initiation of the secondary EM [4]. Current primer design concepts have existed for decades, but have also been the source of both toxic metal emissions and a large number EM failures [5]. For example, most primers consist of a lead-based primary explosives, such as lead styphnate or lead azide [6]. One problem with these lead-based primers is that, during use and disposal, they are responsible for airborne lead emissions that are harmful to both the environment and to the individual using

the EM [6]. Another problem is that when these primers have failed, it has led to operational failures of munitions [7]. Low output energy of these primers is one example of a failure mode that results in hangfires, or delayed initiations [8]. These deficiencies in primer design have inspired research aimed at modifying current primers or eliminating them altogether [9–11].

1.2 Replacing Primer Designs

Over the past few decades, numerous efforts have been made to update and/or replace the primer design for conventional munitions. While several methods have sought to replace the lead-based components within the primers with environmentally friendly ones [12–17], other methods have aimed to replace the primer design altogether with alternative forms of ignition [10, 18]. Some of these methods have included mechanical and optical solutions, including laser ignition [19,20], but electrical ignition has been of particular interest due to low the ignition energy requirements and comparatively short ignition delays [1]. EM that are susceptible to preheating or ignition from these electrically conductive devices typically react to either electrostatic discharge (ESD) or resistive (ohmic) heating [21–23]. Regarding ESD, a common method of transmission is through spark. When a spark delivers a sufficient amount of energy to an ESD sensitive EM, it results in the ignition of the EM [24]. Ohmic heating, may be used as a source of preheating or igniting the EM. When an adequate amount of current is induced in a conductor, such as gold or platinum, it heats up as a function of the input energy [23, 25]. This results in simultaneous thermal heating of the adjacent EM. When preheated to a pre-defined temperature, this adjacent heating has been utilized to enhance the flame speed of energetic materials [26]. Preheating has also proved to be a viable way of sensitizing propellants to thermal decomposition [27]. In addition to preheating, conductive devices may also be used as exploding bridgewires (EBWs), or initiators. When a high current pulse is induced in the conductor, the EBW bursts resulting in a combination of heat and

shock sufficient for detonating secondary explosives [28]. Given that there are multiple ways to utilize conductors with EMs, there may be added benefit to embedding conductive additives into EMs.

1.2.1 Conductive Additives in Energetic Materials

In the past 20 years, electrically conductive additives have been investigated to assess their impact on a wide variety of materials. When these additives have been mixed with other materials, improvements to the materials' mechanical properties, thermal stability and electrical conductivity have resulted [29–31]. While several studies have been performed on a variety of conductive additives, research related to carbon-based additives, such as carbon nanotubes (CNTs), graphene nanoplatelets (GNPs) and carbon black (CB), has shown multiple enhancements to material systems [32, 33]. In energetic materials, some of these enhancements include improved combustion performance, ignition sensitivity, and electrical conductivity [34–37]. For example, the electrostatic discharge (ESD) ignition sensitivity of EM has been influenced through the addition of these conductive materials [38, 39]. With these performance improvements, carbon-based additives have emerged as a potential source for energetic primer replacement.

Carbon-based additives offer a potential solution to primer defects and EM failure. As materials that yield relatively high electrical conductivity due to free flowing electrons in their outer molecular shells, these carbon additives can be preheated directly by way of ohmic heating. If integrated into current EM systems, a 'conductive energetic material' capable of being directly ignited using ohmic heating may result. While the carbon additives were not utilized for this purpose in the study, CNTs have been shown to increase the thermal ignition sensitivity of Al/CuO to a hot wire igniter in previous work [40]. This may have been a result of current flowing from the hot wire through the conductive CNTs, prompting electric and thermal energy to heat up a larger region of the EM than solely the local area influenced by the hot

wire. The work discussed here focuses on creating a conductive energetic material by embedding carbon nanomaterial within the EM and identifying the resulting effects on its energetic performance. The goal of this is to leverage the conductive properties of the additive to allow for direct ohmic heating of the EM. This work also discusses the multi-functionality of these conductive additives when embedded in EM systems, including strain sensing capabilities. Lastly, this work will demonstrate the benefits of selectively depositing conductive additives using additive manufacturing techniques.

1.3 Project Scope and Goals

1.3.1 Conductive Energetic Material Samples

Aluminum/polyvinylidene fluoride (Al/PVDF) is a thermally sensitive fluoropolymer that has been well characterized with regard to its mechanical, thermal, and reactive properties over the past decade [41–45]. The work in Chapter 2 seeks to harness the properties of carbon-based additives within Al/PVDF to provide an alternative ignition source to traditional primer designs. As a thermally ignitable material, the Al/PVDF ignites once it reaches its onset temperature of $\simeq$ 375 °C [44]. Chapter 2 investigates the time to ignition of the Al/PVDF/GNP samples as a function of solids loading of GNP and the voltage applied to the samples. Resistive heating tests were performed using a DC power supply connected directly to the samples. This experiment was performed in hopes of preheating the samples to the point of ignition, leveraging the conductive properties of the GNP as the catalyst for ohmic heating. To inspect the combustion performance of the conductive composite as the solids loading of GNPs increased, differential scanning calorimetry (DSC) and thermal gravimetric analysis (TGA) were performed. These results were compared with a formulation of Al/PDVF with 0% GNP content.

1.3.2 Additively Manufactured Conductive Energetic Composites

As demonstrated in the literature, Al/PVDF is additively manufacturable [44,45]. It has also been well characterized with respect to its material and combustion properties as a printable filament [46,47]. Chapter 3 carries on the successes of Chapter 2, in hopes of merging ohmic heating as a method of pre-heating/ignition with the additive manufacturing of Al/PVDF. Additive manufacturing (AM), more specifically fused filament fabrication (FFF), has several benefits over traditional manufacturing methods. For example, the strict design constraints that govern traditional manufacturing methods are diminished by AM techniques [48]. In addition, dual printed materials can be selectively deposited and merged with one another using AM as the method of manufacturing [49]. This selective deposition could prove to be highly advantageous in EM application and would also be effective in labor reduction when compared with those methods traditionally used to produce bridgewire systems suitable for initiating EMs. From Chapter 2, limitations were evident with respect to both the reactivity of the EM, as well as the electrical conductivity of the conductive EM at lower solids loadings of the carbon additive. Through selective deposition of the conductive and energetic materials using additive manufacturing techniques, their conductive and reactive properties may be conserved.

In Chapter 3, conductive materials are integrated with energetic materials by way of FFF. Prior work involved optimizing the print parameters of Al/PVDF [44]. Using these techniques allowed for the Al/PVDF to be co-printed with commercial conductive filament by utilizing independent dual extrusion (IDEX). IDEX printing enables the two filaments to be printed independently of each other to maintain optimal combustion and conductive properties. A CraftBot 3 was used to co-print the materials outlined in this chapter. The resistive heating tests from Chapter 2 were replicated on samples of Al/PVDF and a conductive graphene-polylactic acid (PLA) filament, to show that ohmic heating could still be used to ignite energetic samples manufactured using AM techniques. The time to ignition during the resistive

heating tests was also measured as a function of applied voltage. This was done in hopes of obtaining a more instantaneous ignition.

Strain gauges, made of the conductive filament, were selectively deposited into Al/PVDF-based flexural test pieces to show that they could be used as strain sensors for structural health monitoring in parallel with being hot wire igniters. In addition to demonstrating multi-functionality, these flexural test specimens demonstrate the integrability and scalability of this method.

2. IMPLEMENTING CARBON NANOFILLERS WITH METAL/FLUOROPOLYMER SYSTEMS FOR CONTROLLED IGNITION

2.1 Introduction

The work in this chapter seeks to replace current primer designs by utilizing a method of ignition for energetic materials that relies on electrical stimuli. Early work in this field has shown several advantages of using carbon-based additives in EM. For example, the literature has shown an increase in thermal conductivity, electrical conductivity, and thermal transport properties as a result of adding CNTs and GNPs to fluoropolymer-based EMs [38, 50]. In parallel, similar studies have looked at the minimum ignition energy of aluminum/metal oxide (such as Al/CuO) through hot wire ignition, but did not involve conductive additives [24]. Prior work was also performed that indicated an increase in the thermal ignition sensitivity of Al/CuO through the addition of CNTs [40]. While these works discuss the capabilities of carbon nanofiller to influence electrical and thermal ignition sensitivity, they do not utilize the carbon nanofiller as a hot wire itself, nor discuss the effects on the reaction rate of the EM as a result of adding these carbon nanofillers.

The challenge still remains to replace primer designs for energetic materials. The work in this chapter makes an effort to achieve this by mixing graphene nanoplatelets (GNPs) with aluminum/polyvinylidene fluoride (Al/PVDF). Specifically, the addition of GNPs resulted in a conductive energetic material, capable of being preheated and ignited using ohmic heating. This capability was assessed by performing resistive heating tests on Al/PVDF/GNP samples. The exothermic reaction of these GNP filled samples were then compared to that of Al/PVDF composites with 0% GNP content to observe potential detrimental effects.

2.2 Experimental Approach

2.2.1 Materials

The conductive energetic material formulations investigated in this chapter involved three base constituents: Aluminum (Al) particles (H3, 4.5 μm diameter spherical particles, Valimet Inc.), polyvinylidene fluoride (PVDF, Kynar 711), and graphene nanoplatelets (GNPs, US-Nano, 95+%, Thickness 2-8 nm, 3-6 layers). Al particles react exothermically with the fluorine in the PVDF when heated to its onset temperature of $\simeq$ 375 °C, classifying it as an energetic material [44]. Micron aluminum particles were chosen over nanoaluminum particles for safety concerns during the mixing procedure. Similar to the research done by Fleck et al., PVDF was chosen due to its low decomposition onset temperature ($\simeq$ 375 °C) [44]. GNPs were used over other commonly used additives, including carbon nanotubes (CNTs) and carbon black (CB), because they posed less respiratory hazards and yielded a higher geometric aspect ratio than that of CNTs and CB, respectively. [32, 37, 51]. This allows for better surface contact between platelets, leading to a percolating network at a lower solids loading.

2.2.2 Material Preparation

The first step, before formulating the conductive energetic samples, was to specify the desired content of each constituent. The mass of each component was dependent on the desired solids loading of GNP. These mass specifications were identified by

$$\underbrace{2x}_{Mass\text{ of GNP}} + \underbrace{0.2(2-2x)}_{Mass\text{ of Al}} + \underbrace{0.8(2-2x)}_{Mass\text{ of PVDF}} = \underbrace{2,}_{Total\text{ Mass}} \tag{2.1}$$

in which x represents the percentage of GNP desired in decimal form (i.e. 0.15 for 15%), and the first, second, and third term represents the mass of GNP, Al, and PVDF, respectively. The term on the right side of the equation is the total mass, in grams, of material mixed into one sample. For safety concerns, this was held at

2 g. Using this equation, a list of all of the variations that were used throughout this chapter was created and is shown in Table 2.1. Previous work has shown that Al/PVDF has viable energetic properties at 20 wt. % of aluminum [44]. To align with this, the aluminum and PVDF in the mixture were intentionally kept at a 20:80 ratio to maintain comparability to the previous work, hence the 0.2 and 0.8 in Equation 2.1. While this equation maintains the ratio between these two constituents, it does not take into account the change in stoichiometry due to the carbon-based additive. A theoretical chemical equation to illustrate how the GNPs react with the Al/PVDF is shown in Equation 2.2. In this example, 4 wt.% GNP is used to calculate the coefficients; but as the solids loading of GNP is varied throughout this chapter, so are the coefficients in the chemical reaction.

$$0.71\mathrm{Al} + 1.20\mathrm{C_2H_2F_2} + 0.33\mathrm{C} \rightarrow 0.71\mathrm{AlF_3} + 0.27\mathrm{HF} + 1.07\mathrm{H_2} + 2.73\mathrm{C} \qquad (2.2)$$

To formulate the samples, PVDF was completely dissolved in a 30 mL vial with a co-solvent of dimethylformamide (DMF) (Anhydrous 99.8% , Sigma Aldrich) and acetone (Sunnyside Specialty Chemicals) to create a polymer precursor. For every 2 g of total material, 15 mL of solvent was used for mixing, 5 mL of DMF and 10 mL of acetone. The amount of solvent mitigated the risk of overheating the sample during mixing in the digital sonifier (Branson Ultrasonics). Once the PVDF was dissolved, the specified amount of GNP were added into the vial, and lastly, the aluminum was added.

After all three solid components were mixed in with the co-solvent, the 30 mL vial containing the solution was then transferred into the digital sonifier such that the sonifier wand was approximately 1 cm from the bottom of the vial. The sonifier was set to mix at an amplitude of 15% for 5 min, to replicate previous Al/PVDF mixing procedures. Once mixing was complete, the mixed solution was poured into a metal weigh tin and left to cure for 48 hr at room temperature.

Early formulations revealed an uneven distribution of the composite mixture, as shown with a 30 % solids loading GNP sample in Figure 2.1. Attempts were made to create a more homogenous mixture; however, these efforts ultimately led to orders

Table 2.1.
The mass of each component of Al/PVDF/GNP based on the weight percentage of GNP.

Batch #	**Wt. %**	**GNP (g)**	**Al (g)**	**PVDF (g)**
0	0.0	0.00	0.400	1.600
1	0.5	0.01	0.398	1.592
2	1.0	0.02	0.396	1.584
3	1.5	0.03	0.394	1.576
4	2.0	0.04	0.392	1.568
5	11.0	0.22	0.356	1.424
6	12.0	0.24	0.352	1.408
7	13.0	0.26	0.348	1.392
8	14.0	0.28	0.344	1.376
9	15.0	0.30	0.340	1.360
10	20.0	0.40	0.320	1.280
11	25.0	0.50	0.300	1.200
12	30.0	0.60	0.280	1.120

of magnitude higher resistance values. This was due to an even dispersion of GNPs throughout the energetic material as opposed to localized agglomerations, meaning that the GNPs were not in close enough proximity for percolation to be achieved. To maintain higher conductivity values for the test samples, the heterogeneous mixtures were used.

2.2.3 Ignition Sample Preparation

Ignition samples were prepped in order to test for the consistency of the ignition of the conductive energetic samples. A three-piece mold was required in order to obtain reliable ignition samples of the materials previously described. A 6.35 mm thick

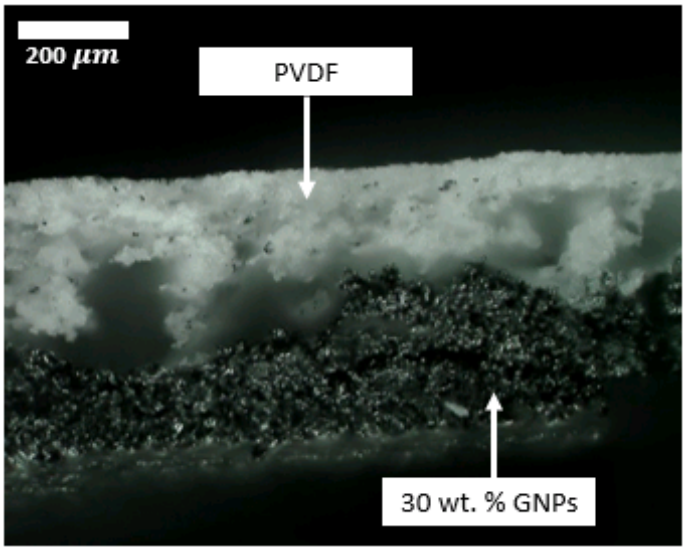

Figure 2.1. Cross-sectional view of a 30 % solids loading Al/PVDF/GNP sample.

Teflon block (McMaster-Carr, Part No. 9266K86) and a weather-resistant EPDM rubber sheet (McMaster-Carr, Part No. 8610K46) were used as the gasket and base, respectively, to formulate the ignition samples as the energetic material dried. Six molds were CNC milled into the Teflon sheet with dimensions of 25.4 mm x 5 mm, with 5 mm rounds on the ends. The third component of the three-piece system was an arbitrary insulation block that was used as a base under the EPDM sheet. Bar clamps were used to hold the system together. After the aforementioned sonication process, a syringe was used to extract $\simeq$ 0.5 mL of solution from the metal weigh tin to transfer to each mold in the apparatus. The molds and other remnants in the metal weigh tin were left idle for 48 hr to allow time for solidification prior to further testing. A visual of this setup is shown in Figure 2.2

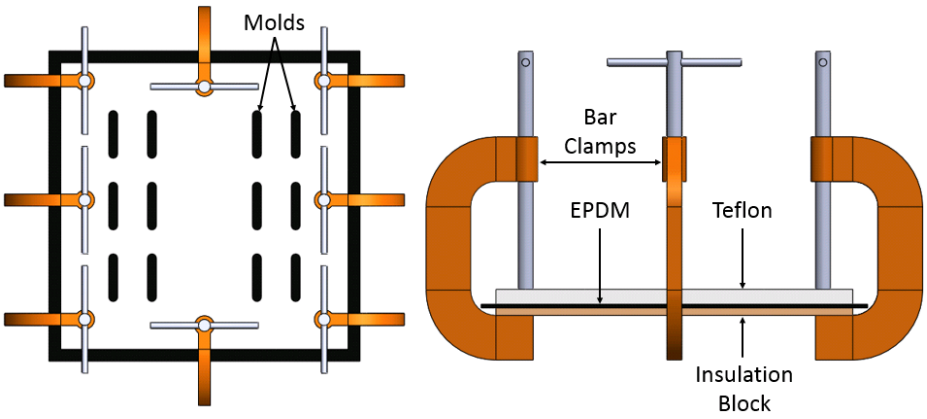

Figure 2.2. Al/PVDF/GNP samples solidifying in a 3-part mold of teflon, EPDM and insulation block held together with bar clamps. The left side is a top view and the right is a side view.

Figure 2.3. Six resistive heating samples of Al/PVDF/GNP at 15% solids loading GNP.

2.2.4 Electrical Resistive Testing

Once the samples solidified, they were carefully extracted and individually connected to a DC power supply (E3634 200 W Power Supply, Allied Electronics & Automation) to apply voltage-limited power to preheat the conductive energetic material. The experimental apparatus is shown in Figure 2.4. Toothless alligator clips were used to connect the power supply to each sample, which reduced contact resistance and prevented unintentional puncture damage to the samples prior to testing. For safety purposes, each test took place within a fume hood with a ceramic tile

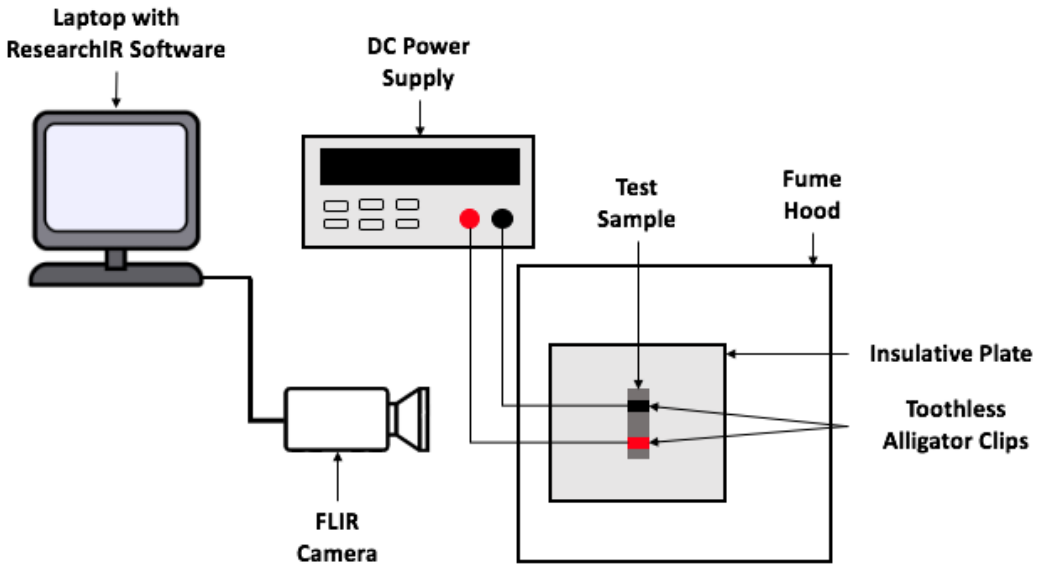

Figure 2.4. The test apparatus used for resistively heating the Al/PVDF/GNP samples.

placed underneath the sample being tested to prevent the reaction from spreading. To gauge the electrical conductivity of each sample, approximate resistance values were obtained by applying 5 V to each sample through the two wires connected to the power supply. The maximum current output from the power supply was used in conjunction with the applied voltage to calculate the resistance. Using Ohm's Law,

$$V = IR, \tag{2.3}$$

in which V, I, and R, represent voltage, current, and sample resistance, respectively, an approximate resistance was calculated for each sample [52]. This procedure was repeated at 10 V. Afterwards, the applied voltage was increased to 20 V to test for the time to ignition of each sample. Through experimentation, 20 V was identified as the minimum ignition voltage that would appreciably heat up the samples, for the range of GNP solids loading samples tested, within 60 s.

2.3 Results and Discussion

In order for an energetic material to be considered for use in application, its exothermic reaction must be repeatable and predictable. In addition, the average time required for the ignition source to preheat the EM must be low, typically within milliseconds. If these performance metrics are not met, it would be unlikely for the ignition method to be approved for functional use. The following results highlight the importance of proper formulation ratios on the success and repeatability of igniting these conductive energetic samples using ohmic heating. Further research, with higher applied voltages, should be conducted to decrease the time to ignition to the microsecond scale.

2.3.1 Electrical Resistance Tests

Initially, solids loadings of GNP between 0.5% - 2% were mixed with Al/PVDF in hopes of significantly increasing the overall electrical conductivity of the energetic material, similar to the extent seen in previous work [38, 40]. These formulations were derived from line items 1-4 in Table 2.1. After the Al/PVDF/GNP mixtures solidified in metal weigh tins, three rectangular strips, with dimensions of $\sim$ 2.5 cm x $\sim$ 1 cm, were cut from each cured composite to take preliminary resistance measurements. These measurements were taken to quantify the effects that incorporating GNPs would have on the conductivity of the energetic material. When measuring the resistances, the probes were kept 1 cm apart from each other, as shown in Table 2.2. While the presence of GNP was noticeable, only localized sections of the energetic samples showed resistive readings due to an uneven dispersion of the GNP during the curing process. As a result, only the lowest measured resistance value is represented for each solids loading of GNP in Table 2.2. Afterwards, the GNP content was increased to allow for an even dispersion of the particles, as well as to produce lower resistances of the Al/PVDF/GNP samples. These formulations are represented as line items 9-12 in Table 2.1.

Table 2.2.
Resistance and conductivity measurements obtained from Al/PVDF samples with low percentage solids loadings of GNP.

GNP (wt. %)	**Length (cm)**	**Width (cm)**	**Height (cm)**	**Resistance (kΩ)**	**Conductivity (μS/cm)**
0.5	1.0	1.0207	0.269	150	1.83
1	1.0	1.035	0.245	40.1	6.32
1.5	1.0	0.816	0.23	5.5	34.1
2	1.0	0.874	0.252	0.441	499

To thoroughly decrease the resistance of the test sample, the GNP solids loading was increased to 15% and estimated resistance measurements were taken using a digital multimeter (DMM). Resistance readings were only present on the base of the sample, with respect to its position during the solidification process. The top of the sample yielded no trace of GNP content due to the settling of the GNP component as the solvent evaporated, as shown in Figure 2.1. When the leads were not in contact with the conductive base, the DMM read OL (open loop), meaning there was no percolation through the sample. To combat this during electrical resistance and ignition testing, the toothless alligator clip connectors were required to be in constant contact with the bottom of the sample to generate the electrical current.

Attempts were made to prevent settling, and therefore the heterogeneity of the sample, in attempt to make the process compatible with additive manufacturing (AM). During the mixing procedure, a hot plate was used to boil the mixture to evaporate the solvent after it had been sonicated. While this technique did result in a more homogenous specimen, the samples' overall conductivities were significantly reduced due to the lower concentrations of GNPs in any specific local areas. In hopes of igniting these samples with as little voltage as possible, the previous formulation technique, without the hot plate, was used to allow for the GNPs to agglomerate on the bottom surface. This allowed for successful electric ignition tests with relatively low applied voltages.

At 15% solids loading, the conductive surface yielded much lower resistance values, (ranging from 71.4 Ω - 263.2 Ω) as compared to those obtained when the solids loading was between 0.5% - 2% (440 Ω - 150 kΩ). With lower resistances, lower power inputs were required to heat up the Al/PVDF/GNP samples to the onset temperature of Al/PVDF ($\simeq$ 375 °C). These resistance values were obtained by applying 5 V to the samples from the DC power supply with the toothless alligator clips spaced 1 cm apart. The resistances were calculated using the voltage input and current output from the power supply in Ohm's Law. This approach was used in hopes of obtaining a more representative resistance measurement at higher sample temperatures. As the applied voltage preheated the conductive material, changes in resistance may have resulted due to the Temperature Coefficient of Resistance (TCR). The TCR refers to the change in resistance of a resistor in ppm with each degree Celsius change in temperature. This process for calculating the resistance values was repeated for the 20%, 25%, and 30% solids loading samples, with six samples at each mass fraction. The resulting resistance values are shown in Figure 2.5, noting that the as GNP solids loading increased, the resistance values were more consistent and decreased. With this range of data, the resistance values ranged from 71.4 Ω - 263.2 Ω for the 15 % solids loading samples, 32.1 Ω - 79.4 Ω at 20 %, 27.0 Ω - 47.2 Ω at 25 %, and 16.7 Ω - 43.1 Ω at 30 %. As the solids loading was increased, percolation became increasingly feasible within the composite, resulting in more consistent resistance values.

The conductivities of these samples, also shown in Figure 2.5, were calculated based on the resistance calculations. The values ranged as high as 0.243 S/cm for one sample at 30% solids loading of GNP, three orders of magnitude higher than the sample with 2 wt.% GNP that was tested previously. Conclusively, the data confirmed that as the solids loading of GNP increased, the conductivity of the samples would also increase.

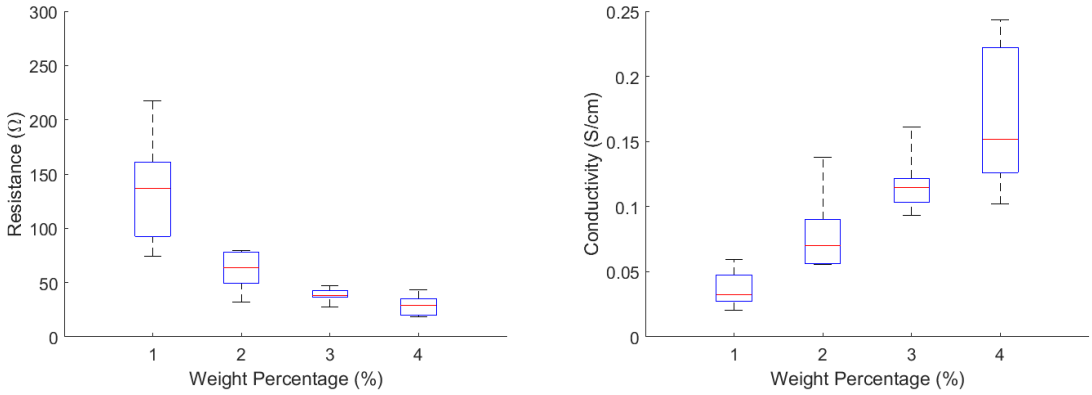

Figure 2.5. Resistance values (left) and calculated conductivity values (right) obtained from six Al/PVDF/GNP samples each at 15%, 20%, 25%, and 30% solids loading GNP, denoted as 1, 2, 3, and 4 on the x-axes, respectively.

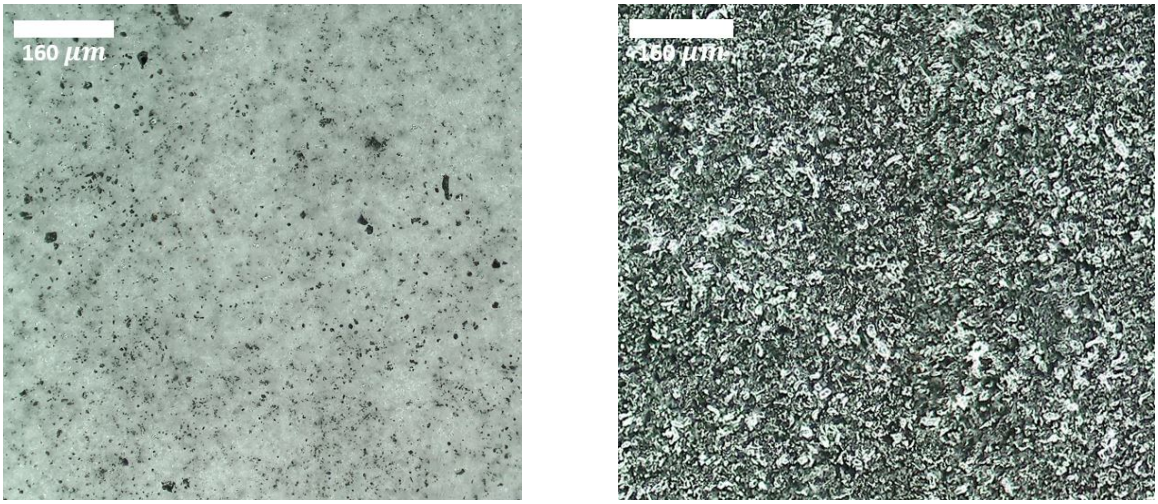

Figure 2.6. Images of the top (left) and bottom (right) of a 30% solids loading Al/PVDF/GNP sample. This demonstrates the heterogeneity of the sample, with the top half of the sample being GNP-lean while the bottom half was GNP-rich.

2.3.2 Cross-Sectional Imaging

To further investigate the settling of the graphene nanoplatelets, cross-sectional images of the samples were imaged using a digital microscope (HIROX KH-8700). As a white substance, PVDF can be readily identified in Figures 2.1 and the left image in Figure 2.6 within the upper portion of the sample. As shown in Figures 2.1 and the right image in Figure 2.6, Al and GNP were mixed primarily towards the bottom half of the samples, with the bottom surface being exceedingly GNP-rich. This uneven distribution may be attributed to the hydrophobic nature of graphene. GNPs are characterized as multiple layers of graphene, which make the compound increasingly hydrophobic and, therefore, resistant to dispersion in solutions [53]. By allowing settling to occur, the GNP-rich surface provides significantly higher conductive properties to the test pieces. Otherwise, a substantially higher amount of voltage would be required to ignite a sample with dispersed GNPs due to higher resistances throughout the sample.

2.3.3 Electric Impulse Ignition Tests

After the electrical resistance was calculated, the applied voltage was increased in 5 V increments until ignition occurred. 20 V was identified as the applied voltage amount that would consistently preheat and ignite the conductive energetic samples. Per observation, it was noted that as the output temperature of a given sample increased above $\simeq$ 160 °C, the sample began to deform due to the melting point of PVDF ($\simeq$ 175 °C) being approached. This deformation was one of the primary sources of inconsistency between samples. As deformation occurred, the alligator clips would shift in position, causing unrepeatable fluctuations (either increasing or decreasing) in the maximum temperature output. This melting typically affected the data when 10 V and 15 V were applied to the samples with greater amounts of GNP content (25% and 30% solids loading), as they generated higher current that

heated the material above $\simeq$ 175 °C, but not high enough to reach the ignition onset temperature.

When 20 V was applied, a sufficient power output was produced to ignite the material. This process was repeated for 15%, 20%, 25%, and 30% solids loading samples in hopes of decreasing the time to ignition as the solids loading of GNP increased. The results of each ignition test are shown in Table 2.3. As expected, the lower solids loading GNP samples took longer to heat up as compared to the ones with higher solids loading, indicating that higher concentrations of GNP lead to greater conductivity, thus allowing for the samples to preheat faster when the applied voltage was held constant.

Quantitatively, the 15%, 20%, and 25% solids loading samples ignited in average times of 7.2, 2.2 and 1.8 seconds, respectively. It was noted that the mechanical properties of the samples degraded as excess GNPs were added to Al/PVDF. As the GNP content increased, the test pieces became exceedingly brittle and often times broke prior to testing. This is indicative of the first column of Table 2.3; as the GNP solids loading increased, the number of samples that remained intact from the six formulated samples decreased. It was also observed that the 30% solids loading samples did not ignite (DNI), even though they heated up to the onset temperature of Al/PVDF (375 °C). Since GNPs are carbon based, they are considered a fuel; however, the GNP particles do not exothermically react with the PVDF oxidizer due to the GNPs' high melting point of 3,600 °C (per the Safety Data Sheet from US-Nano). This high melting point inhibited the nanoplatelets from deflagrating at the ignition onset temperature for Al/PVDF. As excess GNPs were added to the Al/PVDF, the stoichiometry was impacted and caused the Al/PVDF/GNP to be exceedingly fuel rich. This compromised the combustion performance of the energetic material, revealing a trade off when trying to achieve the goal of creating conductive energetic materials. To quantify the impact that adding these nanofillers had on the energetic properties of Al/PVDF, it was necessary to perform a combustion analysis

to compare the exothermic reaction of these conductive energetic samples to that of Al/PVDF.

Table 2.3.
The time to ignition of conductive energetic samples at 15%, 20%, 25%, and 30% solids loading GNP.

No. of Samples	GNP (wt. %)	Avg. Time to Ignition (s)	Std. Dev. (s)
5	15	7.2	1.32
3	20	2.2	0.74
3	25	1.8	0.59
2	30	DNI	N/A

2.3.4 Energetic Performance of the Conductive Energetic Material

From the previous data, it was conclusive that as the solids loading of GNP increased, the greater effect it would have on the conductivity. This makes the conductive additives more attractive as an ignition system. However, at these higher solids loadings, the combustion performance was being sacrificed. These contradictions led to an investigation of the energetic performance of the conductive energetic material using digital scanning calorimetry (DSC) and thermal gravimetric analysis (TGA). With this approach, 15% solids loading samples were tested to analyze the heat flow patterns that the Al/PVDF/GNP sample exemplified in comparison to the work reported in previous literature with neat Al/PVDF [44]. The comparison is shown below in Figure 2.7.

Similarities from each test included the slight endothermic reactions at 175 °C and 660 °C, which represent the melting points of PVDF and aluminum, respectively, and the peak exothermic reaction occurring at $\simeq$ 575 °C. The maximum heat flow generated from the Al/PVDF was approximately 26.9 W/g. The 15% solids loading GNP sample had a 19.3% reduction in its maximum exotherm, with a maximum heat

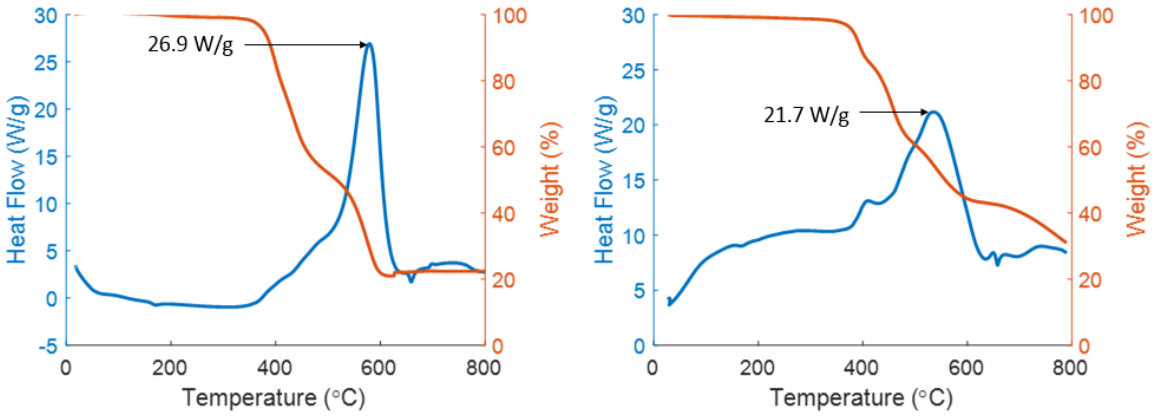

Figure 2.7. A comparison between DSC/TGA performed on Al/PVDF from Fleck et al. (left) and on an Al/PVDF sample with 15% solids loading GNP (right).

flow of 21.7 W/g. This reduction can be attributed to the addition of GNPs altering the fuel/oxidizer stoichiometry.

After this analysis, attempts were made to lower the GNP solids loading to find the threshold that would allow for ignition with 20 V applied during the electrical resistive and ignition tests. Samples at 11, 12, 13, and 14% solids loading GNP were prepared using the component formulations mentioned earlier in Table 2.1. After obtaining resistances measurements, 20 V were applied to each sample. There was no ignition at 11 or 12% solids loading GNP, but at 13%, ignition occurred in two of the six samples tested, crediting the inconsistent dispersion of GNP throughout each specimen. Since it was assumed that the energetic performance would be greater with less GNP content, a DSC scan was also performed on this solids loading to quantify the combustion. The data collected from this DSC test showed minimal change in the results, with a maximum exotherm of 22.0 W/g. At those lower GNP concentrations, ignition could still be obtained through higher applied voltages.

2.4 Conclusions

This chapter provided a foundation for using embedded conductive additives to directly preheat and ignite energetic materials. The conductive properties of these additives allow them to be ohmically, or thermally, heated, thus enabling the controlled ignition of the energetic material without the need of a Nichrome wire or other traditional ignition sources. Various amounts of GNPs were incorporated into Al/PVDF to quantify the time required for an applied voltage to preheat the Al/PVDF/GNP sample to the ignition temperature of Al/PVDF. The concentration of the carbon additives influence the overall conductivity of the material, which correlated to a decrease in time required for constant voltage to be applied prior to ignition. It was noted that as the content of GNPs increased, the sample resistance decreased. However, it was also observed that as the GNP content increased, there were negative effects on the energetic performance of the Al/PVDF composite. Further experimentation should be performed that varies the solids loadings to effectively characterize a formulation that results in negligible impact to the exothermic reaction of the energetic material. Alternatively, future work could look to decouple the ignition system and energetic material but have them co-located using additive manufacturing. This may allow for the trade offs experienced in this chapter to be bypassed by maintaining the integrity of both the EM and the conductive additive. Further investigation is also needed to reduce the time to ignition of the conductive energetic material and yield a more instantaneous ignition. Resistive heating tests with higher applied voltage may yield more favorable results for time to ignition for the formulations described in this work. The results of these investigations would increase the likelihood of direct ohmic heating ignition being more widely used in application.

3. ADDITIVE MANUFACTURING OF CONDUCTIVE/REACTIVE COMPOSITE MATERIAL SYSTEMS

3.1 Introduction

The work in this chapter takes an alternative approach for fabricating conductive energetic materials and related composites than that of Chapter 2. Fused Filament Fabrication (FFF), an additive manufacturing method, is used in this chapter as the replacement method of fabrication. Prior work has developed print parameters and optimized a process for additively manufacturing Al/PVDF [44, 45, 54]. Recent studies have been conducted to quantify the mechanical and combustion properties of printed Al/PVDF [46], while others have sought to understand the role that the aluminum solids loading plays on the print viscosity of the EM [47]. Through these studies, Al/PVDF has been well characterized as an additively manufacturable energetic fluoropolymer. Given these printing capabilities, this work seeks to print the Al/PVDF with a conductive polymer to recreate the geometries from Chapter 2 in a more reliable manner.

Recent work has studied conductive filament material and has identified potential options for integration in various applications. For example, commercial conductive filaments, including Conductive PLA (Proto-Pasta), Conductive Graphene PLA (BlackMagic3D), and Electrifi (Multi3D), were compared to conductive paint and conductive fabric for their strain sensing capabilities [55]. Custom conductive filaments, including "carbomorph" (a custom composite made of carbon black and polycaprolactone), PVDF/multi-walled carbon nanotubes (MWCNTs), and CNT yarn, have also been fabricated and used in research as functional conductive filaments [56–58]. These conductive filaments have been used for several purposes, including capacitive

buttons and 'smart vessels' [56], but most commonly are valued as embedded strain gauges for static and dynamic sensing [59–62].

Combining the shortcomings of the previous chapter along with the prior work in the field of printed conductive materials, the experiments performed in this chapter seek to accomplish two goals. First, this work seeks to leverage commercially available conductive filament as an ignition source for the Al/PVDF by selectively depositing them adjacent to one another. Selective deposition allows for concentrated amounts of conductive filament to be integrated with Al/PVDF for ignition purposes, while maintaining viable energetic properties. Secondly, the work in this chapter looks to utilize the integrated conductive filament to monitor the structural integrity of the EM through an embedded strain gauge. Accomplishing these two goals would give the conductive filament multi-functional usage as an embedded strain sensor and as a hot wire igniter.

3.2 Experimental Section

3.2.1 Materials

The experiments outlined in this chapter use several different 3D-printable filaments. A list of these filaments can be found in Table 3.1. One of these was a custom homogenous filament comprised of aluminum (Al) particles (H3, 4.5 μm diameter spherical particles, Valimet Inc.), polyvinylidene fluoride (PVDF, Kynar 711), and graphene nanoplatelets (GNPs, US-Nano, 95+%, Thickness 2-8 nm, 3-6 layers). This filament was made using formulation techniques from Chapter 2 and was used as a baseline for comparing the resistances of the other conductive filaments in this chapter. Two commercial filaments, Polylactic Acid (PLA Gold 1, CraftBotUSA, 1.75 mm, 1.0 kg) and FLUORX^{TM} PVDF (3DXTECH, 1.75 mm, 500 g), were used to rapid prototype preliminary inert parts and optimize print parameters prior to printing with energetic Al/PVDF. In addition, commercial conductive filaments, including Conductive PLA [Proto-Pasta (PP), MatterHackers, 1.75 mm, 500 g], Con-

ductive Graphene PLA [Black Magic (BM), Graphene Supermarket, 1.75 mm, 100 g], and Electrifi (EF) [Multi3D, 1.75 mm, 100 g] were also used as potential filaments for printing in this chapter. Each conductive filament was kept in a dry environment using 3D Printer Filament Boxes (Katamco). All of the filaments were printed using the CraftBot 3, an independent dual extrusion (IDEX) 3D printer.

Table 3.1.
List of filaments used in this chapter and their uses.

Filament	**Commercial/Custom**	**Type of Filament**
Al/PVDF	Custom	Energetic
Al/PVDF/GNP	Custom	Conductive and energetic
Black Magic (BM)	Commercial	Conductive
Electrifi (EF)	Commercial	Conductive
FLUORX^{TM} PVDF	Commercial	Inert
Polylactic Acid (PLA)	Commercial	Inert
Proto-Pasta (PP)	Commercial	Conductive

3.2.2 Al/PVDF/GNP Filament Preparation

Pellet Preparation

Before using the commercial filament for dual printing with Al/PVDF, efforts were made to print with Al/PVDF/GNP as a custom conductive filament at both 15% and 25% solids loading GNP. The fabrication method to prep the energetic composite (outlined in Chapter 2, Section 2.2) was used, but instead of being extracted into molds after the sonication process, the composite was left to solidify in the metal weigh tins for 48 hrs. Replicating the process of Fleck et al., the resultant $\sim$ 2 mm thick film that was cut into pellets (approximately 2 mm x 2 mm x 2 mm) and fed

into the Filabot Extruder. 20 grams of pellets were made per formulation for filament fabrication.

Filament Fabrication

A filament extruder (Filabot Extruder EX2, Filabot) was used to extrude the conductive energetic material into a 3D printable filament. The extruder was pre-heated to 195 °C for 30 min with the extrusion screw operating at a rate of 35 rpm. The Filabot extruder presented safety hazards when operating with energetic materials due to the required application of both heat and pressure in a confined chamber to extrude the filament. As a safety precaution, the filament extrusion process was operated remotely in a separate room. The test setup is shown in Figure 3.1.

Prior to vacating the room, the energetic pellets were poured in one side of a custom dual funnel that was centered over the opening of the extruder. Purge pellets were also poured in the second opening of the funnel. This funnel was blocked by a trap door, which could be operated remotely. Once the room was vacated, the remote-operated door was retracted to allow the energetic pellets to be released into the extruder. After about 10 min of extrusion with the energetic pellets, the remote-operated door was retracted again, allowing the energetic material to be replaced by inert purge pellets (Extruder Cleaning Purge Compound, Filabot) without any human interaction. Due to the remote set up, a tensioner could not be used, which made it difficult to control the diameter of the filament. To maintain a filament diameter below 1.75 mm (the diameter requirement for the CraftBot 3), a 1.60 mm nozzle was placed on the extruder. After the extrusion was complete, only sections of consistent diameter were kept and used for further testing. This extrusion process was also used to formulate the Al/PVDF filament used in this chapter.

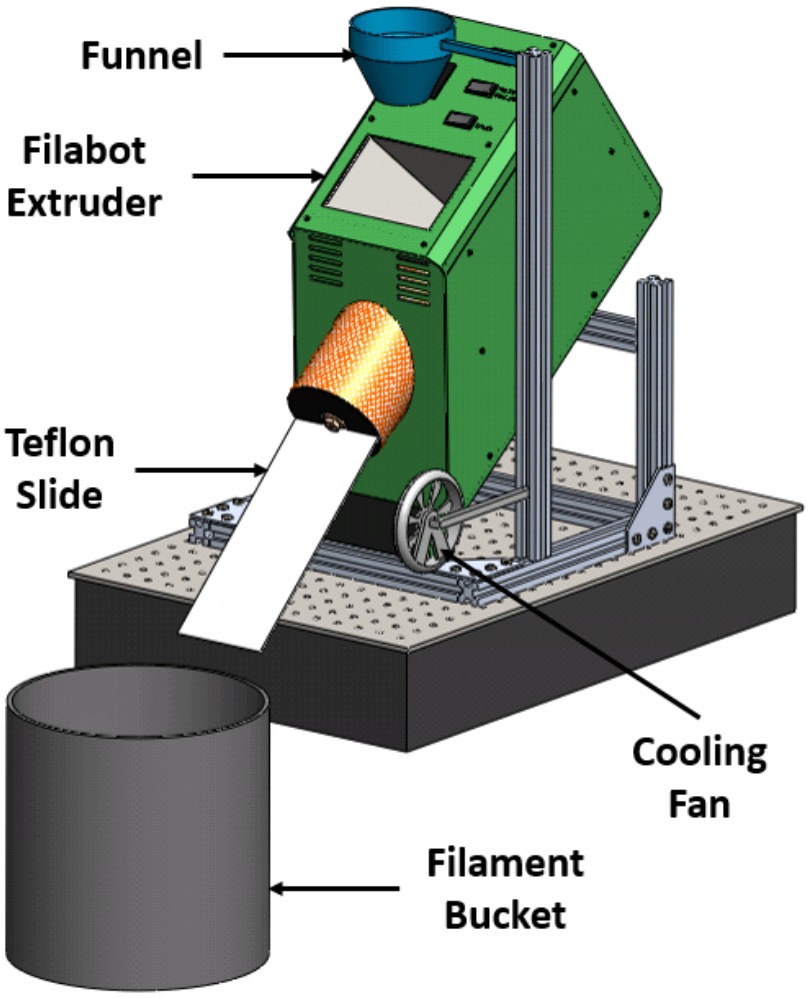

Figure 3.1. Test apparatus for energetic filament extrusion.

3.2.3 Sample Printing and Key Metrics

Each filament that was printed required a unique set of parameters to yield successful prints. Samples were printed successfully using a 99% aligned rectilinear infill pattern at 90°. Key parameters that were modified for printing the energetic material included print speed and print temperature. The PVDF, Al/PVDF, and Al/PVDF/GNP filaments required slower print speeds at higher temperatures to avoid clogging in the nozzles, due to both the low melt flow index of PVDF and

the addition of aluminum and carbon-based particles. The extrusion multiplier also needed to be manually adjusted on the CraftBot 3 to gain more traction when printing with these materials. In addition, it was necessary to adjust the diameter size of the energetic filament in the slicer software (Slic3r) to match the actual diameter, as a result of the remote extrusion process producing undersized filament. Each filament, except the Electrifi filament, was printed on BuildTak Original 3D Printing Surface (BuildTak) to maintain adhesion between the filament and the build plate. The Electrifi filament was significantly more adhesive than the other filaments, resulting in difficulties when attempting to remove it from the BuildTak; therefore, the Electrifi filament was either printed on top of other printed material or directly on the build plate. A table of key print parameters can be found below in Table 3.2.

Table 3.2.
A list of key print parameters that were used when printing with the filaments of interest here.

Parameter	Al/PVDF	Al/PVDF/GNP	PVDF	PLA	BM	EF	PP
Print Temperature (°C)	245	245	245	220	220	140	220
Bed Temperature (°C)	110	110	110	60	50	20	60
Print Speed (mm/s)	10	10	15	30	20	20	20
Print Direction (°)	90	90	90	Any	Any	Any	Any
BuildTak (Y/N)	Yes	Yes	Yes	Yes	Yes	No	Yes

3.2.4 Electrical Resistive Testing

The tests performed in this section mirror those described in Chapter 2, Section 3.1 of this document. Test samples (25.4 mm x 5 mm x 1 mm) were fabricated using the CraftBot 3 printer. Initial samples were created with three layers of PLA filament that was then printed with two identical layers of Proto-Pasta on top. These inert samples represented a successful composite print that yielded the conductive properties that could be expected when printing conductive energetic test pieces.

Successful ignitions of the conductive energetic test pieces would indicate that the goal of achieving ohmic heating ignition was possible when additive manufacturing techniques were used to integrate the conductive material with the EM.

Prior to performing resistive heating tests, the resistance values of these samples were measured by taking 4-wire resistance measurements using a Keysight Multimeter (34465A, Keysight). Toothless alligator clips were used and were spaced 5 mm apart from each other, along the length of the sample, to take the measurements, as shown in Figure 3.2. This process was repeated for the other two conductive filaments, Black Magic and Electrifi. Al/PVDF/GNP samples were also printed with similar dimensions to compare resistance values of the formulations in Chapter 2 to the dual printed samples. These results are provided and explained in the Results and Discussion section of this chapter.

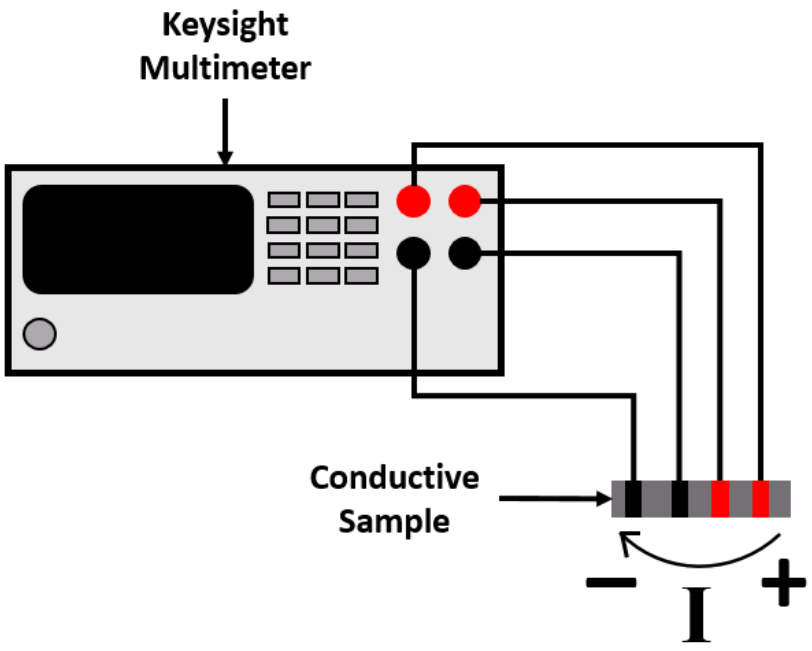

Figure 3.2. The 4-wire resistance setup used for calculating the resistances of the conductive test samples.

To better simulate conductive energetic material printing, PVDF was dual printed with both Black Magic (BM) and Electrifi (EF) conductive filaments, as they yield superior conductive properties to that of Proto-Pasta (PP), as shown in Table 3.3. These test pieces were connected to a DC power supply (E3634 200 W Power Supply, Allied Electronics & Automation). 25 V were applied to both the PVDF/BM and PVDF/EF samples to heat them up to the ignition onset temperature of Al/PVDF ($\simeq$ 375 °C). The resistance values of the Black Magic filament were similar to those of the Al/PVDF/GNP samples at 15% and 20% GNP solids loading (Samples 9 and 11 in Table 2.1 in Chapter 2, Section 2.2), therefore 25 V was assumed to be capable of preheating the printed filament to the ignition onset temperature of Al/PVDF. These tests were repeated from 30 V - 50 V, increasing in 5 V increments, to quantify the effects of higher voltage on the time to ignition onset temperature of the samples. A thermal camera (FLIR Model: A6507, FLIR) was used to document the change in temperature of the samples during the tests. This process was replicated using Al/PVDF with the conductive filaments.

3.2.5 Multi-functional Conductive Filament

For practical use as a hot wire igniter, successful ignition would need to occur as a result of integrating the conductive filament with larger EM samples. In addition, prior work has shown that the viability of these conductive filaments as potential strain sensors when embedded in materials [59, 61, 62]. Larger printed samples were created to examine if both of these contributions could result from the conductive filament when integrated with larger amounts of EM. A flexural test specimen (ASTM C1161-18 Configuration C) made of Al/PVDF with an embedded strain gauge of Black Magic was printed. A visual of this flexural specimen is shown in Figure 3.3.

After dual printing this flexural specimen, two tests were conducted with it. First, a cyclical 3-point bending test was performed on the flexural test specimen using a mechanical tester (ESM1500, Mark-10). To prep the sample for this test, wires were

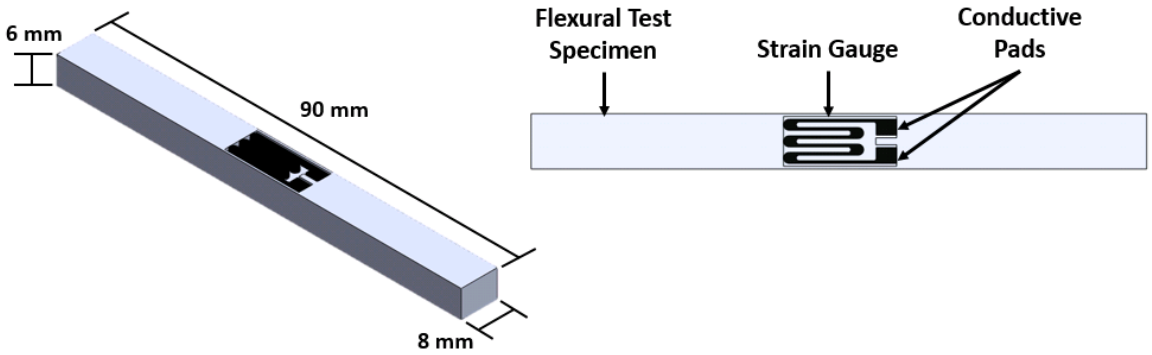

Figure 3.3. CAD model of a flexural test specimen with an embedded strain gauge.

attached to the conductive pads on the printed strain gauge using a silver conductive epoxy (Conductive Adhesive for Electronics 7661A13, McMaster Carr) and was left to cure for 24 hrs. Once solidified, the wires were connected to a Keysight Multimeter to record the change in resistance of the strain gauge as loads were applied to the flexural specimen. A LabView data acquisition code was written to document the data from the multimeter. The flexural test specimen was displaced between 0.5 mm - 1.5 mm at a rate of 1 mm/min for seven cycles. From this test, the resulting applied loads and corresponding resistance values were obtained. The second experiment was a resistive heating test using methods similar to those outlined in Chapter 2, Section 3.3 of this paper. The wires that were connected to the flexural specimen were wired to a DC power supply (1685B Switching Mode Power Supply, BK Precision) to ohmically heat the sample by applying 60 V. This power supply was used in contrast to the former because it yielded a higher power output, 300 W, compared to 200 W. This power output was necessary as the resistance of the strain gauge was higher than that of the resistive test samples due to the length of the strain gauge from one pad to the other ($\sim$ 74 mm).

3.3 Results and Discussion

The work in Chapter 2 proved that conductive additives could be used to provide an alternative source of ignition for energetic materials. However, these results came at the expense of the reactive properties of the EM. In order for ohmic heating with conductive materials to be a favorable method of igniting EM, the energetic performance cannot be severely compromised. With the advancement of additive manufacturing, multi-material printing serves as a prominent method of selectively depositing separate materials into one piece without chemically mixing them. As an added benefit of selective deposition, conductive filament may be of use as a strain sensor in addition to an alternative ignition source when integrated with EM. The work in this section utilizes Fused Filament Fabrication to formulate test samples to obtain these goals.

3.3.1 Resistance Comparisons and Material Selection

The samples discussed here were printed to prove that multi-material printing with a conductive filament was feasible, and to compare the resistance values of the dual printed samples with that of the homogenous conductive energetic filament, Al/PVDF/GNP. These results are shown on the log-scale graph in Figure 3.4. The resistances of the dual printed samples of PLA/Proto-Pasta were orders of magnitude lower than that of the energetic composite filaments. Because of these results, only multi-material prints were used for further tests and commercial conductive filaments beyond Proto-Pasta were sought.

There are multiple commercially available conductive filaments, and several have already been well characterized for their conductive properties [55, 58]. Both Conductive Graphene PLA [Black Magic (BM)] and Electrifi (EF) were acquired and measured to determine their resistance values using the techniques in the previous paragraph. Both the filament and printed samples were measured to quantify these values pre- and post-print. These results were compared to those of Proto-Pasta and

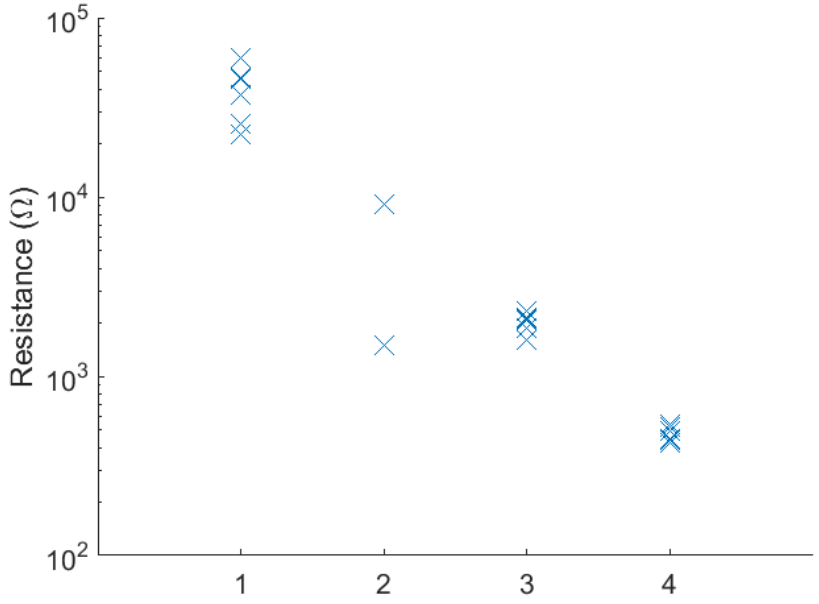

Figure 3.4. Results from the 4-wire resistance test. On the x-axis, "1" and "3" are the Al/PVDF/GNP filaments at 15 wt.% and 25 wt.% GNP content, respectively, "2" is the Al/PVDF/GNP printed test piece at 15 wt.% GNP content, and "4" is the printed sample of PLA/Proto-Pasta.

are outlined in Table 3.3. From the table, it was concluded that it would be more advantageous to use the Black Magic and the Electrifi filaments during the resistive heating tests, as they yielded better conductive properties than that of the Proto-Pasta. Its worth noting that the Electrifi filament resistance varied significantly when heated past 60 °C, the melting point of Electrifi (per the Multi3D website). This is potentially a result of the copper particles realigning during the melt phase, thus altering the resistive readings. During printing, the print temperature of the filament was 140 °C, therefore a realignment of the copper particles may have caused inconsistencies in the resistance values between the printed samples. This may have been a source of the large standard deviation of the measured resistance values shown in Table 3.3.

Table 3.3.
Comparing measured resistance and conductivity values of the commercial conductive filaments.

Sample Type		Sample Size	Avg. Resistance (Ω)	Avg. Conductivity (Ω/cm)	Std. Dev. (Ω/cm)
Proto-Pasta	**Filament**	5	244.2	0.172	0.0055
	Printed	5	497.2	0.0423	0.0038
Electrifi	**Filament**	5	0.634	77.7	31.8
	Printed	5	7.402	9.72	9.63
Black Magic	**Filament**	5	41.0	1.05	0.224
	Printed	5	174.0	0.117	0.0547

3.3.2 Electrical Resistance Tests

Once the conductive filaments were selected, resistive heating tests were performed on samples of PVDF/Black Magic (BM) and PVDF/Electrifi (EF). All of the samples were printed with dimensions of 25.4 mm x 5 mm x 1 mm with three 0.2 mm layers of PVDF with two 0.2 mm layers of conductive filament printed on top. It was necessary to print PVDF as the base layer for the printed parts, as it requires a heated bed temperature of 110 °C to resist warping of the material. Using toothless alligator clips to connect from the DC power supply to the samples, 25 V were applied to test if the samples could be ohmically heated to the ignition onset temperature of Al/PVDF ($\simeq$ 375 °C). The results of these tests are shown in Figure 3.5. The PVDF/EF samples consistently heated up to $\sim$ 100 °C and shortly thereafter settled to a temperature of $\sim$ 42 °C. This was a result of the resistance of the Electrifi increasing after its melting point ($\sim$ 60 °C) had been exceeded, per the Safety Data Sheet provided by Multi3D. However, the PVDF/BM samples yielded favorable results, proving that Black Magic could consistently be preheated to the onset ignition temperature of Al/PVDF using ohmic heating.

This process was repeated for the PVDF/BM samples with applied voltages from 30 V - 50 V, in 5 V increments, to quantify this time at higher voltages. Three samples were tested for each voltage interval. The goal was to show the potential

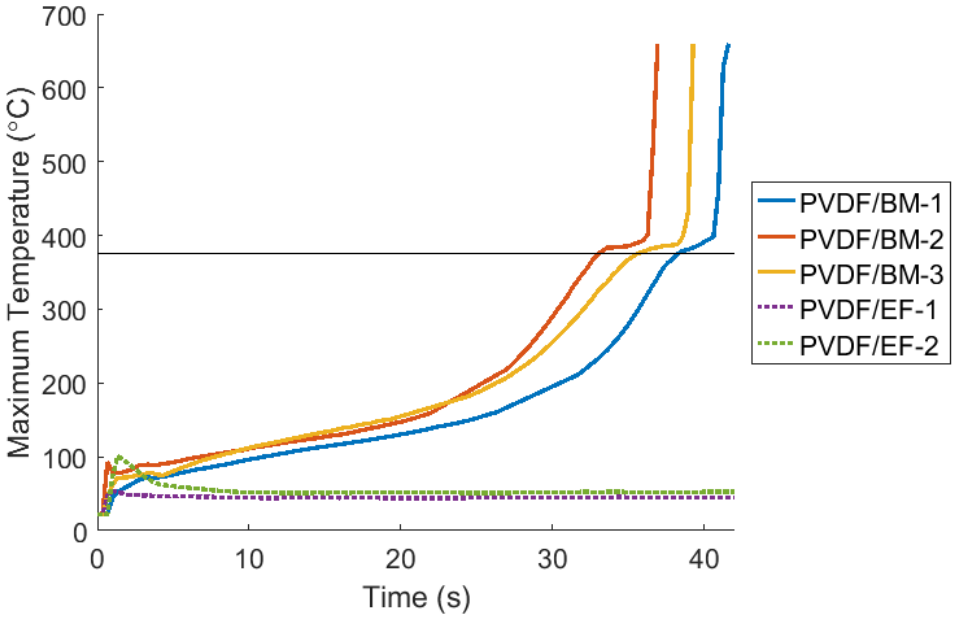

Figure 3.5. Resistive heating tests at 25 V on PVDF/BM and PVDF/EF test samples.

for ignition to occur within milliseconds using ohmic heating as higher voltages were used. Figure 3.6 shows the time to ignition onset temperature of Al/PVDF as a function of applied voltage. As the voltage increased, the time to ignition onset temperature exponentially decreased, resulting in an average preheat time of 4.5 s at 50 V. Since these inert dual printed samples yielded positive results, this experiment was performed once more using Al/PVDF in place of PVDF to test the ability to ohmically heat conductive energetic prints to ignition.

The Al/PVDF/BM samples were printed using the same dimensions as the other test samples in this chapter. Resistive heating tests were conducted on these samples using a DC power supply and applying various voltages from 25 V - 50 V. Three samples were tested at each interval in hopes of replicating the results from Figure 3.6. There was a decrease in time to ignition onset temperature as the applied voltage was increased for the conductive energetic Al/PVDF/BM, as there was for the inert

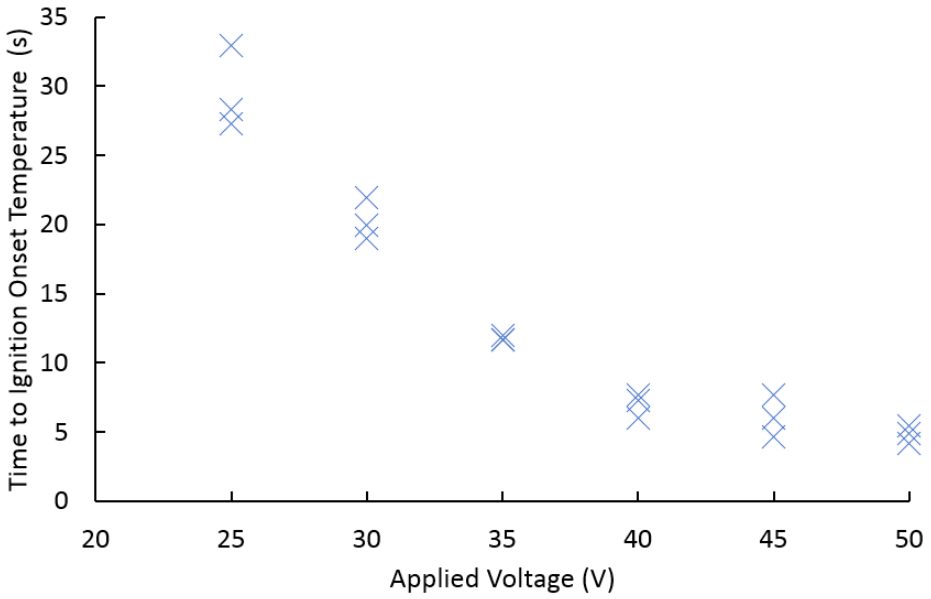

Figure 3.6. The time to ignition onset temperature of Al/PVDF ($\simeq$ 375 °C) at various applied voltages as obtained from the PVDF/BM test samples.

test samples. A graph is shown in Figure 3.7 that compares the two sample sets. It was observed that the Al/PVDF/BM samples reached the ignition onset temperature for Al/PVDF at a faster rate than that of the PVDF/BM samples at every voltage interval. This may have been due to the Al content in the Al/PVDF prompting a faster reaction as the temperature of the BM increased. A table with the averages and standard deviations of each interval is referenced in Table 3.4. From this table it is shown that as the applied voltage increased the standard deviation for time to ignition decreased for both sample sets. This may be due to the varied resistance values of the samples having less impact on the reaction at higher voltage inputs. As shown in the power formula for Ohm's law

$$P = \frac{V^2}{R}, \tag{3.1}$$

in which V is the applied voltage and R is the resistance of the sample, as the applied voltage increases, the resistance of the sample contributes less to the total power

output [63]. Further investigation should be performed to correlate the heating rate of Al/PVDF/BM to the Al content in the energetic material. From the data, it is conclusive that as the amount of applied voltage is increased, the time for ohmic heating ignition of conductive EM decreases. This was supported given the average time to ignition onset temperature at 50 V was 1.493 s for Al/PVDF/BM. A separate study may also be performed that investigates the application of high voltage to the conductive EM in hopes of yielding a more instantaneous ignition.

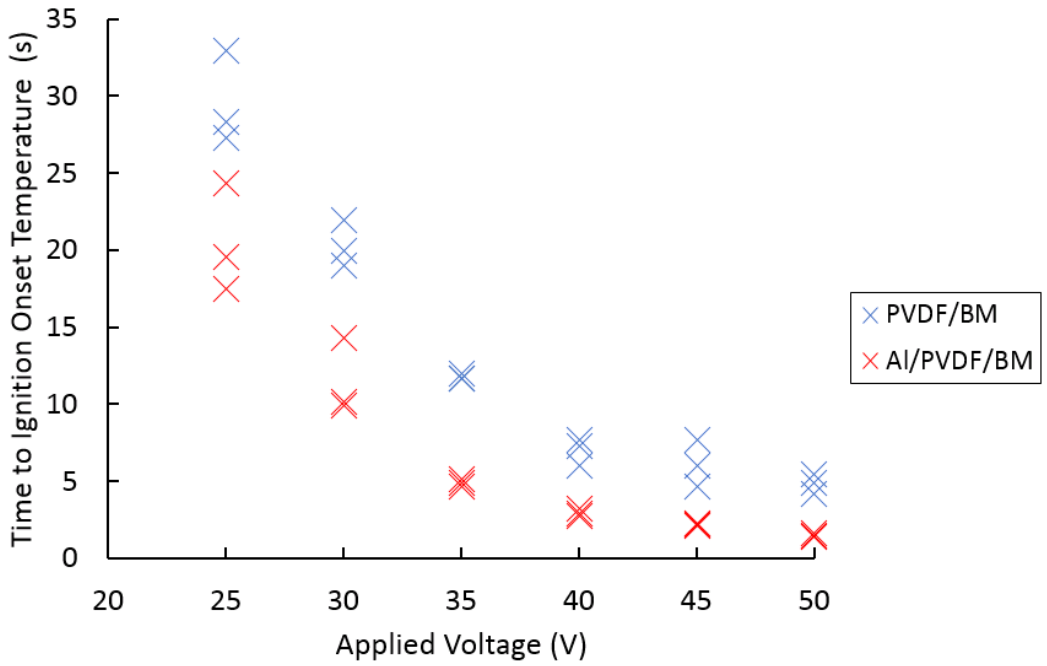

Figure 3.7. The time to ignition onset temperature of Al/PVDF ($\simeq$ 375 °C) at various voltage applications as obtained from both the inert PVDF/BM and the energetic Al/PVDF/BM test samples.

3.3.3 Flexural Tests with Embedded Strain Gauges

To characterize the Black Magic as a strain sensor, a cyclical three-point bending test was performed on the flexural test piece that displaced the specimen between 0.5 mm and 1.5 mm for seven intervals at 1 mm/min in each direction. A pre-load

Table 3.4.
The averages and standard deviations for times to ignition onset temperature of Al/PVDF for inert PVDF/Black Magic (BM) and Al/PVDF/BM resistive heating samples.

Sample Type		**25 V**	**30 V**	**35 V**	**40 V**	**45 V**	**50 V**
PVDF/BM	Average (s)	29.505	20.294	11.760	6.983	6.117	4.850
	Standard Deviation (s)	3.018	1.514	0.185	0.888	1.522	0.650
Al/PVDF/BM	Average (s)	20.461	11.447	4.870	2.919	2.198	1.493
	Standard Deviation (s)	3.502	2.466	0.241	0.243	0.080	0.130

of 5 N was applied to the sample to calibrate the tester with the specimen prior to starting the test. The acquired data for both the resultant force values and the corresponding resistance values is outlined below in Figure 3.8. The data showed

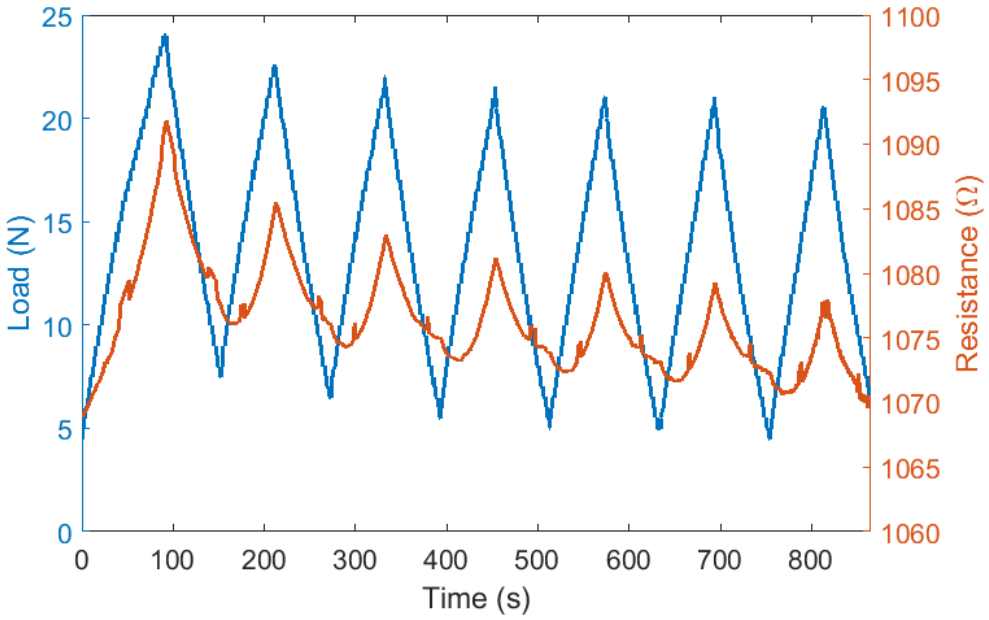

Figure 3.8. The resultant load applied to the flexural specimen and corresponding resistance readings from the printed strain gauge during the cyclical three-point bending test.

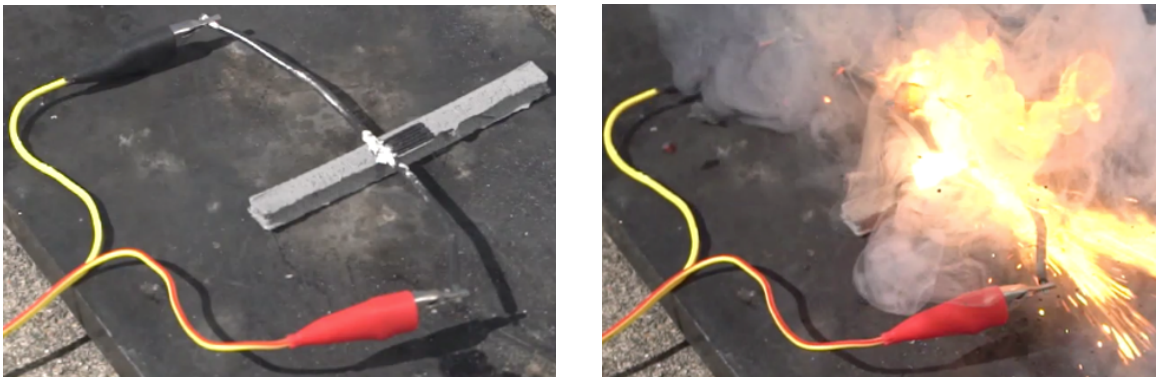

Figure 3.9. Pre- and post-ignition images of the flexural test specimen due to ohmic heating.

that an increase in the deflection of the beam (which prompted the increase in load) resulted in a repetitive increase in resistance from the printed strain gauge. This was an indicator that the Black Magic served as a viable strain gauge for monitoring the structural health of the EM. The resistance of the strain gauge was also observed to be a couple orders of magnitude higher than that of the resistive heating samples that were formulated in Section 3.1 of this chapter. This statistic was expected due to the difference in geometry of the strain gauge compared to the rectangular resistive test pieces. The distance along the strain gauge from one conductive pad to the other was $\sim$ 74 mm, yielding much higher resistance values than that of the resistive heating test pieces since resistance is calculated as

$$R = \frac{\rho L}{A}, \tag{3.2}$$

where ρ is the resistivity of the material, L is the sample length, and A is the cross sectional area of the sample [64]. The increase in length was likely the leading factor in the increased resistance readings. A commercial strain gauge may also be integrated onto the flexural test specimen for comparison purposes in future experimentation, but the purpose of this work was to demonstrate the multi-functionality of the conductive additive with energetic materials.

3.3.4 Ohmic Heating of the Flexural Test Specimen

After the three-point bending test was completed, the second experiment that was performed on the flexural specimen was a resistive heating test by routing the conductive wires from the specimen to a DC power supply. 60 V were applied to the embedded strain gauge and it ohmically heated to the ignition temperature of Al/PVDF, similar to the resistive heating tests performed earlier this chapter. The higher voltage was used to accommodate for the higher resistance of the sample ($\sim$ 1070 Ω), as shown in Figure 3.8. Before and after images of this reaction are shown in Figure 3.9. As observed, ignition of the Al/PVDF was successfully achieved by way of ohmic heating using the embedded printed strain gauge, proving that it is plausible to integrate it with heat-sensitive EM as an embedded hot wire igniter.

3.3.5 Conclusion

The work in this chapter took the concept of ohmic heating ignition from Chapter 2 of this document and implemented additive manufacturing techniques as the method of formulation for the conductive energetic materials. The goal in this chapter was to prove the viability of integrating conductive filament with energetic material through multi-material printing of the materials into one part. In addition, this chapter also discussed the multi-functional use of the conductive filament by demonstrating its usefulness as a strain sensor. Through the experiments performed here, the conductive filament demonstrated both strain sensing and igniter capabilities, indicating multiple benefits for integrating conductive material in EM systems.

Further experimentation should be implemented to research the effects of aluminum content on the heating rate of the conductive energetic material prior to ignition. Resistive heating tests were performed on both inert samples of PVDF/Black Magic, as well as on the energetic Al/PVDF/Black Magic samples. A clear contrast between the time to ignition onset was evident from the data comparison at each voltage interval, crediting the addition of the 20% aluminum content as the source of

the increased rate of reaction. Future research may also involve high voltage applications to the conductive material in hopes of achieving a more instantaneous ignition of the EM.

4. CONCLUSION

Ohmic heating was proven to be a viable way of igniting energetic materials when conductive additives were integrated with them. Two strategies were used in this document to formulate conductive energetic materials. Various mass solids loadings of graphene nanoplatelets (GNPs) were mixed with a reactive mixture of Al/PVDF to formulated molded test samples. These samples were successfully ignited using ohmic heating until the solids loading of the GNPs reached 30%. This prompted an investigation on the impact of the GNPs on the energetic properties of the Al/PVDF. Findings indicated that mixing the conductive additive with the Al/PVDF had adverse effects on the energetic properties. As a result, an alternative manufacturing method was pursued in hopes of maintaining these properties. A CraftBot 3 was used to print both the Al/PVDF and Conductive Graphene PLA (Black Magic) independently of each other into one part. Ohmic heating was then used to ignite these conductive energetic samples at various applied voltages, yielding a negative correlation between the applied voltage and time to ignition for the sample. Subsequently, the multi-material printing was scaled to produce an energetic flexural test specimen with an embedded strain gauge made of the Black Magic filament. The strain gauge was subjected to two tests: to show that it was capable of igniting the larger energetic sample, and to demonstrate its capabilities of being used as an embedded strain sensor for the energetic material. After performing a cyclical three-point bending test and recording the change in resistance values of the printed strain gauge, the Black Magic was proven to be viable as a strain sensor. Afterwards, 60 V were applied to the strain gauge, resulting in the ignition of the flexural test specimen. In addition to proving that ohmic heating could be applied to scaled energetic material systems, these tests also demonstrated the multi-functionality of integrating conductive additives with energetic materials.

REFERENCES

REFERENCES

[1] S. Lundgaard, S. Ng, D. Cahill, J. Dahlberg, D. Ruan, N. Cole, P. Stoddart, and S. Juodkazis. Towards safer primers: A review. *Technologies*, 7(4):75, October 2019.

[2] K. Engelen and M.H. Lefebvre. Properties of gas-generating mixtures related to different fuel and oxidizer compositions. *Propellants, Explosives, Pyrotechnics*, 28(4):201–209, August 2003.

[3] N.K. Bourne. On the laser ignition and initiation of explosives. *Proceedings of the Royal Society of London. Series A: Mathematical, Physical and Engineering Sciences*, 457(2010):1401–1426, June 2001.

[4] J. Sabatini and K. Oyler. Recent advances in the synthesis of high explosive materials. *Crystals*, 6(1):5, December 2015.

[5] D.K. Han, M.G. Pecht, D.K. Anand, and R. Kavetsky. Energetic material/ systems prognostics. In *2007 Annual Reliability and Maintainability Symposium*, Orlando, FL, USA, 2007. Institute of Electrical and Electronics Engineers.

[6] J. Fronabarger, M. Williams, and M. Bichay. Environmentally acceptable alternatives to lead azide and lead styphnate. In *43rd AIAA/ASME/SAE/ASEE Joint Propulsion Conference & Exhibit*, Cincinnati, OH, USA, July 2007. American Institute of Aeronautics and Astronautics.

[7] F.S. Atchison and N.J. Asher. Primer selection for small arms ammunition. Technical report, Institute for Defense Analysis, Alexandria, VA, USA, November 1970.

[8] L.J. Bement, C. Holmes, J. McGrory, and M.L. Schimmel. An investigation to improve quality evaluations of primers and propellant for 20 mm munitions. Technical report, NASA Langley Research Center, Hampton, VA, USA, February 1997.

[9] L. Guindon, D. Lepage, and J.-P. Drolet. Non-toxic primers for small caliber ammunition. US Patent 6,620,267, September 2003.

[10] R. Yalamanchili and M.E. Ellis. Environmentally friendly percussion primer. US Patent 7,980,178 B1, July 2011.

[11] P. Ostrowski, M. Bichay, T. Allen, V. Sanders, and S. Son. Recent accomplishements in MIC primer development at NSWC/Indian Head. In *41st AIAA/ASME/SAE/ASEE Joint Propulsion Conference & Exhibit*, Tucson, AZ, USA, July 2005. American Institute of Aeronautics and Astronautics.

[12] J.W. Fronabarger, M.D. Williams, W.B. Sanborn, J.G. Bragg, D.A. Parrish, and M. Bichay. DBX-1 - a lead free replacement for lead azide. *Propellants, Explosives, Pyrotechnics*, 36(6):541–550, December 2011.

[13] J.W. Fronabarger, M.D. Williams, W.B. Sanborn, D.A. Parrish, and M. Bichay. KDNP - a lead free replacement for lead styphnate. *Propellants, Explosives, Pyrotechnics*, 36(5):459–470, October 2011.

[14] R. Brewer, P. Dixon, S. Ford, K. Higa, and R. Jones. Lead free electric primer. Technical report, Defense Technical Information Center, Fort Belvoir, VA, USA, October 2011.

[15] K.T. Higa. Energetic nanocomposite lead-free electric primers. *Journal of Propulsion and Power*, 23(4):722–727, July 2007.

[16] P.P. Ostrowski, J.A. Puszynski, M.M. Bichay, and T.M. Allen. Nano energetics for US navy percussion primer applications. In *The 2006 Annual Meeting*, Trondheim, Norway, 2005. Norwegian University of Science and Technology.

[17] P. Ostrowski and M. Bichay. Al/MoO3 MIC primer evaluation tests. II - delay cartridges. In *36th AIAA/ASME/SAE/ASEE Joint Propulsion Conference and Exhibit*, Las Vegas, NV, USA, July 2000. American Institute of Aeronautics and Astronautics.

[18] Y. Kagawa, M. Arifuku, S. Maeda, and H. Mukunoki. Initiatorless electric detonator. US Patent 2008/0190316 A1, August 2008.

[19] L. De Yong, T. Nguyen, and J. Waschl. Laser ignition of explosives, pyrotechnics and propellants: A review. Technical report, Defence Science and Technology Organisation, Melbourne, Victoria, Australia, May 1995.

[20] M. Lavid, S.K. Gulati, and W.R. Lempert. Laser ignition of ball powder (nitrocellulose base). In *OE/LASE '94*, Los Angeles, CA, USA, March 1994. The International Society for Optics and Photonics.

[21] W.L. Shaw, D.D. Dlott, R.A. Williams, and E.L. Dreizin. Ignition of nanocomposite thermites by electric spark and shock wave. *Propellants, Explosives, Pyrotechnics*, 39(3):444–453, June 2014.

[22] T.A. Baginski. Discharge insensitive electro-explosive devices. US Patent 6, 192,802 B1, February 2001.

[23] A. Nicollet, G. Lahiner, A. Belisario, S. Souleille, M. Djafari-Rouhani, A. Estève, and C. Rossi. Investigation of Al/CuO multilayered thermite ignition. *Journal of Applied Physics*, 121(3):034503, January 2017.

[24] C. Weir, M.L. Pantoya, G. Ramachandran, T. Dallas, D. Prentice, and M. Daniels. Electrostatic discharge sensitivity and electrical conductivity of composite energetic materials. *Journal of Electrostatics*, 71(1):77–83, February 2013.

[25] C.S. Staley, C.J. Morris, R. Thiruvengadathan, S.J. Apperson, K. Gangopadhyay, and S. Gangopadhyay. Silicon-based bridge wire micro-chip initiators for bismuth oxide–aluminum nanothermite. *Journal of Micromechanics and Microengineering*, 21(11):115015, November 2011.

[26] Y. Kochar, S. Vaden, T. Lieuwen, and J. Seitzman. Laminar flame speed of hydrocarbon fuels with preheat and low oxygen content. In *48th AIAA Aerospace Sciences Meeting Including the New Horizons Forum and Aerospace Exposition*, Orlando, FL, USA, January 2010. American Institute of Aeronautics and Astronautics.

[27] V. R. Pai Verneker, K. Kishore, and G. Prasad. Effect of preheating on the burning rate of solid propellants. *AIAA Journal*, 14(9):1330–1331, September 1976.

[28] M. T. Hedges and W. B. Freeman. Special grade RDX for exploding bridge wire initiators. *Industrial & Engineering Chemistry Product Research and Development*, 6(2):124–126, June 1967.

[29] A. L. G. Saad, H. A. Aziz, and O. I. H. Dimitry. Studies of electrical and mechanical properties of poly(vinyl chloride) mixed with electrically conductive additives. *Journal of Applied Polymer Science*, 91(3):1590–1598, June 2003.

[30] B. Huang, X. Chen, and X. Shu. Effects of electrically conductive additives on laboratory-measured properties of asphalt mixtures. *Journal of Materials in Civil Engineering*, 21(10):612–617, October 2009.

[31] Y. Cui, C. Liu, S. Hu, and X. Yu. The experimental exploration of carbon nanofiber and carbon nanotube additives on thermal behavior of phase change materials. *Solar Energy Materials and Solar Cells*, 95(4):1208–1212, April 2011.

[32] C. Basavaraja, G.T. Noh, and D.S. Huh. Chemically modified polyaniline nanocomposites by poly(2-acrylamido-2-methyl-1-propanesulfonicacid)/graphene nanoplatelet. *Colloid and Polymer Science*, 291(12):2755–2763, 2013.

[33] M. Rashad, F. Pan, A. Tang, and M. Asif. Effect of graphene nanoplatelets addition on mechanical properties of pure aluminum using a semi-powder method. *Progress in Natural Science: Materials International*, 24(2):101–108, 2014.

[34] K. Kappagantula, M.L. Pantoya, and E.M. Hunt. Impact ignition of aluminum-teflon based energetic materials impregnated with nano-structured carbon additives. *Journal of Applied Physics*, 112(2):024902, July 2012.

[35] K Kappagantula, J. Cano, and M. Pantoya. Combustion performance improvement of energetic thin films using carbon nanotubes. In *51st AIAA/SAE/ASEE Joint Propulsion Conference*, Orlando, FL, USA, 2015. American Institute of Aeronautics and Astronautics.

[36] A. Bach, P. Gibot, L. Vidal, R. Gadiou, and D. Spitzer. Modulation of the reactivity of a WO3/Al energetic material with graphitized carbon black as additive. *Journal of Energetic Materials*, 33(4):260–276, October 2015.

[37] Q.-L. Yan, M. Gozin, F.-Q. Zhao, A. Cohen, and S.-P. Pang. Highly energetic compositions based on functionalized carbon nanomaterials. *Nanoscale*, 8(9):4799–4851, 2016.

[38] E.S. Collins, B.R. Skelton, M.L. Pantoya, F. Irin, M.J. Green, and M.A. Daniels. Ignition sensitivity and electrical conductivity of an aluminum fluoropolymer reactive material with carbon nanofillers. *Combustion and Flame*, 162(4):1417–1421, 2015.

[39] R. Steelman, B. Clark, M.L. Pantoya, R.J. Heaps, and M.A. Daniels. Desensitizing nano powders to electrostatic discharge ignition. *Journal of Electrostatics*, 76:102–107, 2015.

[40] K.H. Poper, E.S. Collins, M.L. Pantoya, and M.A. Daniels. Controlling the electrostatic discharge ignition sensitivity of composite energetic materials using carbon nanotube additives. *Journal of Electrostatics*, 72(5):428–432, October 2014.

[41] W. Zhou, J. Zuo, and W. Ren. Thermal conductivity and dielectric properties of Al/PVDF composites. *Composites Part A: Applied Science and Manufacturing*, 43(4):658–664, April 2012.

[42] J.B. DeLisio, C. Huang, G. Jian, M. Zachariah, and G. Young. Ignition and reaction analysis of high loading nano-Al/fluoropolymer energetic composite films. In *52nd Aerospace Sciences Meeting*, National Harbor, MD, USA, January 2014. American Institute of Aeronautics and Astronautics.

[43] Z. Wang, W. Zhou, X. Sui, and L. Dong. Enhanced dielectric properties and thermal conductivity of Al/CNTs/PVDF ternary composites. *Journal of Reinforced Plastics and Composites*, 34(14):1126–1135, July 2015.

[44] T.J. Fleck, A.K. Murray, I.E. Gunduz, S.F. Son, G.T.-C. Chiu, and J.F. Rhoads. Additive manufacturing of multifunctional reactive materials. *Additive Manufacturing*, 17:176–182, 2017.

[45] D.N. Collard, M. McClain, T. Fleck, N. Rahmann, J. Rhoads, T. Meyer, and S. Son. Solid propellant with embedded additively manufactured reactive components. In *AIAA Propulsion and Energy 2019 Forum*, Indianapolis, IN, USA, August 2019. American Institute of Aeronautics and Astronautics.

[46] H. Wang, M. Rehwoldt, D.J. Kline, T. Wu, P. Wang, and M.R. Zachariah. Comparison study of the ignition and combustion characteristics of directly-written Al/PVDF, Al/Viton and Al/THV composites. *Combustion and Flame*, 201:181–186, March 2019.

[47] F.D. Ruz-Nuglo and L.J. Groven. 3-D printing and development of fluoropolymer based reactive inks. *Advanced Engineering Materials*, 20(2):1700390, 2018.

[48] A. Bandyopadhyay and S. Bose. *Additive Manufacturing, Second Edition*. CRC Press, Milton, 2019.

[49] Z. Sun and L.F. Velasquez-Garcia. Monolithic FFF-printed, biocompatible, biodegradable, dielectric-conductive microsystems. *Journal of Microelectromechanical Systems*, 26(6):1356–1370, December 2017.

[50] K. Kappagantula and M.L. Pantoya. Experimentally measured thermal transport properties of aluminum/polytetrafluoroethylene nanocomposites with graphene and carbon nanotube additives. *International Journal of Heat and Mass Transfer*, 55(4):817–824, January 2012.

[51] J. Howard. Current intelligence bulletin 65: Occupational exposure to carbon nanotubes and nanofibers. Technical report, National Institute for Occupational Safety and Health, Cincinnati, OH, USA, April 2013.

[52] R. Cammack, T. Atwood, P. Campbell, H. Parish, A. Smith, F. Vella, and J. Stirling. *Oxford Dictionary of Biochemistry and Molecular Biology, Second Edition*. Oxford University Press, Oxford, New York, USA, 2006.

[53] G. Wang, B. Wang, J. Park, J. Yang, X. Shen, and J. Yao. Synthesis of enhanced hydrophilic and hydrophobic graphene oxide nanosheets by a solvothermal method. *Carbon*, 47(1):68–72, January 2009.

[54] J.A. Bencomo, S.T. Iacono, and J. McCollum. 3D printing multifunctional fluorinated nanocomposites: Tuning electroactivity, rheology and chemical reactivity. *Journal of Materials Chemistry A*, 6(26):12308–12315, 2018.

[55] M. Al-Rubaiai, R. Tsuruta, T. Nam, U. Gandhi, and X. Tan. Direct printing of a flexible strain sensor for distributed monitoring of deformation in inflatable structures. In *ASME 2019 Conference on Smart Materials, Adaptive Structures and Intelligent Systems*, Louisville, KY, USA, September 2019. American Society of Mechanical Engineers.

[56] S.J. Leigh, R.J. Bradley, C.P. Purssell, D.R. Billson, and D.A. Hutchins. A simple, low-cost conductive composite material for 3D printing of electronic sensors. *PLoS ONE*, 7(11):e49365, 2012.

[57] J.M. Gardner, G. Sauti, J.W. Kim, R.J. Cano, R.A. Wincheski, C.J. Stelter, B.W. Grimsley, D.C. Working, and E.J. Siochi. Additive manufacturing of multifunctional components using high density carbon nanotube yarn filaments. Technical report, NASA Langley Research Center, Hampton, VA, USA, 2016.

[58] A. Almazrouei, R.A. Susantyoko, C.-H. Wu, I Mustafa, A. Alhammadi, and S. Almheiri. Robust surface-engineered tape-cast and extrusion methods to fabricate electrically-conductive poly(vinylidene fluoride)/carbon nanotube filaments for corrosion-resistant 3D printing applications. *Scientific Reports*, 9(1):9618, 2019.

[59] J.J. Ku-Herrera, F. Avilés, and G.D. Seidel. Self-sensing of elastic strain, matrix yielding and plasticity in multiwall carbon nanotube/vinyl ester composites. *Smart Materials and Structures*, 22(8):085003, 2013.

[60] J. Gooding and T. Fields. 3D printed strain gauge geometry and orientation for embedded sensing. In *58th AIAA/ASCE/AHS/ASC Structures, Structural Dynamics, and Materials Conference*, Grapevine, TX, USA, January 2017. American Institute of Aeronautics and Astronautics.

[61] B.J. Ouellette. In-situ printing of conductive polylactic acid (cPLA) strain sensors embedded into additively manufactured parts using fused deposition modeling. Technical report, Los Alamos National Laboratory, Santa Fe, NM, USA, 2018.

[62] M. Maurizi, J. Slavič, F. Cianetti, M. Jerman, J. Valentinčič, A. Lebar, and M. Boltežar. Dynamic measurements using FDM 3D-printed embedded strain sensors. *Sensors*, 19(12):2661, 2019.

[63] H.R. Panchal and D.K. Kanchan. Electrical switching in potassium-borovanadate-iron glasses. *Turkish Journal of Physics*, 23(6):969–976, June 1997.

[64] R.L. Parker and A Krinsky. Electrical resistance-strain characteristics of thin evaporated metal films. 34(9):2700–2708, June 2004.